

Adaptive Mesh Refinement Method for Predicting Three-Dimensional Turbulent Flow

Akarapol Meesit¹, Ekachai Juntasaro², Varangrat Juntasaro¹
and Jack Asavanant³

¹Department of Mechanical Engineering, Faculty of Engineering,
Kasetsart University, Bangkok 10900, Thailand,
Phone: (02)9428555 ext 1829, Fax: (02)5794576, Email: fengvrj@ku.ac.th

²School of Mechanical Engineering, Institute of Engineering,
Suranaree University of Technology, Nakhon Ratchasima 30000, Thailand,
Phone: (044)224410-2, Fax: (044)224411, Email: junta@sut.ac.th

³Department of Mathematics, Faculty of Science,
Chulalongkorn University, Bangkok 10330, Thailand,
Phone: (02)2185141, Fax: (02)2552287, Email: ajack@chula.ac.th

Abstract

An Adaptive Mesh Refinement method (AMR) is presented for predicting turbulent flow in a three-dimensional domain. The low-Reynolds-number linear $k-\varepsilon$ turbulence model of Launder and Sharma [4] is employed to predict turbulent flow. In this paper, AMR is the local refinement method of the active type that relies on high numerical errors or gradient. The Richardson extrapolation is employed to estimate the truncation error. The computer program developed is based on the finite volume method. The SIMPLE algorithm is used to numerically solve this flow problem. It is found that AMR can speed up the computing time significantly when compared to the non-uniform fine-grid with the same grid size. The results obtained agree well with the experimental data of Prasad and Koseff [3].

Keywords: AMR, Truncation error, Cavity.

1. Introduction

Recently, for the rapid advance of computer technology in hardware and software, computational fluid dynamics (CFD) has become a practical tool for analysis of fluid physics and in engineering designs [5]. However, the numerical solution of fluid problem is often obtained with the slow rate of convergence. The need for the fast rate of convergence makes the adaptive mesh refinement more attractive.

The local refinement technique is developed by Berger [1] for a system of hyperbolic partial differential equations. Moreover, this method is extended to a system of elliptic partial differential equations by Caruso [2] who described the application of AMR in steady incompressible laminar flow. Adaptive grids can simplify

solutions to problems that need refinement only in the small regions. Those refined regions depend on numerical errors or gradients and employ the Richardson extrapolation to estimate truncation errors. The resulting numerical solution is as accurate as a non-uniform fine-grid calculation but use less computing time.

The adaptive mesh refinement method is employed in the present work for predicting three-dimensional turbulent flow. The numerical result of turbulent incompressible cavity flow using the low-Reynolds-number linear $k-\varepsilon$ turbulence model of Launder and Sharma [4] is obtained and compared with the experimental data of Prasad and Koseff [3]. The objective of this work to present that this method is accurate and speeds up the computing time significantly.

2. Governing Equations and Numerical Method

2.1 Governing Equations

The governing equations are the Reynolds-averaged continuity and Navier-Stokes equations for steady three-dimensional turbulent incompressible flow. It can be written in the general Cartesian coordinates as:

$$\frac{\partial}{\partial x_j}(\rho u_j) = 0 \quad (1)$$

$$\frac{\partial}{\partial x_j}(\rho u_i u_j) = \frac{\partial}{\partial x_j}(\tau_{ij} - \rho \overline{u'_i u'_j}) - \frac{\partial p}{\partial x_i} \quad (2)$$

$$\tau_{ij} = \mu \left(\frac{\partial u_i}{\partial x_j} + \frac{\partial u_j}{\partial x_i} \right) \quad (3)$$

$$-\overline{\rho u_i' u_j'} = \mu_t \left(\frac{\partial u_i}{\partial x_j} + \frac{\partial u_j}{\partial x_i} \right) - \frac{2}{3} \delta_{ij} (\rho k) \quad (4)$$

where τ_{ij} is the laminar-stress tensor, μ_t is the eddy viscosity, k is the kinetic energy of turbulence, δ_{ij} is the Kronecker delta ($\delta_{ij} = 0$ for $i \neq j$ and $\delta_{ij} = 1$ for $i = j$) and the term $-\overline{\rho u_i' u_j'}$ is called the Reynolds-stress tensor which can be expressed using the Boussinesq assumption [7], [9].

2.2 Turbulence Model

The transport equations of turbulence kinetic energy k and its rate of dissipation ε are solved right down to the wall so that the wall function is not needed. The $k - \varepsilon$ model takes the following form:

$$\frac{\partial}{\partial x_j} (\rho k u_j) = \frac{\partial}{\partial x_j} \left[\left(\mu + \frac{\mu_t}{\sigma_k} \right) \frac{\partial k}{\partial x_j} \right] - \overline{\rho u_i' u_j'} \frac{\partial u_i}{\partial x_j} - \rho \varepsilon - \rho D \quad (5)$$

$$\begin{aligned} \frac{\partial}{\partial x_j} (\rho \varepsilon u_j) = & \frac{\partial}{\partial x_j} \left[\left(\mu + \frac{\mu_t}{\sigma_\varepsilon} \right) \frac{\partial \varepsilon}{\partial x_j} \right] - C_{\varepsilon 1} f_{\varepsilon 1} \frac{\varepsilon}{k} \left(\overline{\rho u_i' u_j'} \frac{\partial u_i}{\partial x_j} \right) \\ & - \rho C_{\varepsilon 2} f_{\varepsilon 2} \frac{\varepsilon^2}{k} + \rho E \end{aligned} \quad (6)$$

where the eddy viscosity, the model constants, the damping functions and the extra terms are provided as follows:

$$\mu_t = \rho C_\mu f_\mu \frac{k^2}{\varepsilon} \quad (7)$$

$$\sigma_k = 1.0, \sigma_\varepsilon = 1.3, C_\mu = 0.09, C_{\varepsilon 1} = 1.44, C_{\varepsilon 2} = 1.92, f_{\varepsilon 1} = 1.0$$

$$D = \frac{2\mu}{\rho} \left(\frac{\partial \sqrt{k}}{\partial x_i} \right)^2 \quad (8)$$

$$E = \frac{2\mu}{\rho} \frac{\mu_t}{\rho} \left(\frac{\partial^2 u_i}{\partial x_k \partial x_m} \right)^2 \quad (9)$$

$$f_{\varepsilon 2} = 1 - 0.3 \exp(-\text{Re}_t^2) \quad (10)$$

$$\text{Re}_t = \frac{\rho k^2}{\mu \varepsilon} \quad (11)$$

2.3 Numerical Method

The governing equations are discretized by the finite-volume method. Using the SIMPLE algorithm and the collocated-grid arrangement, all properties are stored at the cell-center points. The Rhie and Chow interpolation is used to avoid the coupling problem between velocity and pressure field. It can be written in the general form as follows:

$$\frac{\partial}{\partial x_j} (\rho u_j \phi) = \frac{\partial}{\partial x_j} \left(\Gamma \frac{\partial \phi}{\partial x_j} \right) + S^\phi \quad (12)$$

where ϕ is the general dependent variable, Γ is the effective diffusion coefficient and S^ϕ is the source/sink term of ϕ . The convection and the diffusion terms are discretized using the upwind and central differencing schemes respectively. The re-arranged discretized equation can be written as:

$$A_p \phi_p = \sum_{nb} A_{nb} \phi_{nb} + S^\phi \quad (13)$$

where A is the coefficient and S^ϕ is the general source/sink term.

3. Principle of Adaptive Mesh Refinement

The adaptive mesh refinement method is the local refinement method of the two-level active type that relies on high numerical errors or gradient. This method starts from the calculation for solution on both the double grid and the coarse grid. The refined regions can be generated from the estimation of truncation error. Boundary conditions and initial guesses on the refined regions are interpolated from the base grid solution. After that, the solution on the refined regions are restricted to the base grid. The solution transfer between two levels is done by the Taylor series interpolation.

Algorithm of the active method is given as follows:

1. Set up the base grid G_k and the double grid G_{k-1}
2. Calculate the solution on G_k and the double grid
3. Estimate the truncation error on G_k
4. Generate refined regions G_{k+1}
5. Restrict the solution from G_{k+1} to G_k
6. Calculate the base grid correction
7. Calculate the base grid solution
8. Update the boundary values for G_{k+1} by interpolating the solution from G_k
9. Check for convergence
10. If converged, stop; otherwise continue
11. Go to (5)

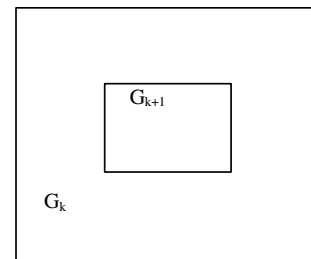


Figure 1. Notation for two-level active solution

4. Error Estimation

For any general elliptic partial differential equation

$$L \phi = F \quad (14)$$

where L is the difference operator, ϕ is the unknown variable, F is the right-hand-side

In this section, the Richardson extrapolation is used to estimate the solution error and the truncation error. This technique assumes that the solution error can be expressed in terms of a Taylor series [2], that is,

$$e(h, x) = u(0, x) - u(h, x) = h^p F(x) + h^q G(x) + \dots \quad (15)$$

where $u(0, x)$ is the exact solution, h is the mesh size and p is the order of the method. The solution error is different at all grid levels. Therefore, the double grid size creates the solution error as.

$$e(2h, x) = u(0, x) - u(2h, x) = 2^p h^p F(x) + 2^q h^q G(x) + \dots \quad (16)$$

The estimation of the solution error is done by subtracting (16) from (15) and then dividing the result by $2^p - 1$:

$$\begin{aligned} \tilde{e}(h, x) &= \frac{u(h, x) - u(2h, x)}{2^p - 1} \\ &= h^p F(x) + h^q \left(\frac{2^q - 1}{2^p - 1} \right) G(x) + \dots \end{aligned} \quad (17)$$

The operator form of the truncation error is defined as the residual obtained by subtracting the exact solution of the differential equation ($u(0, x)$), with the difference equation.

$$\begin{aligned} L_h[u(h, x)] &= f \\ \tau(h, x) &= L_h[u(0, x)] - f \\ \tau(h, x) &= L_h[u(0, x)] - L_h[u(h, x)] \end{aligned} \quad (18)$$

Consequently, the relationship between the solution error and the truncation error is obtained by:

$$\tilde{\tau}(h, x) = L_h[\tilde{e}(h, x)] \quad (19)$$

where $\tilde{\tau}$ is the estimated truncation error and \tilde{e} is the estimated solution error. The active solution is calculated on a multilevel grid system. Therefore, the estimated truncation error is calculated only at nodes not contained on a finer grid level. The error estimation in the active method is coupled between the solution error and the truncation error. The solution error estimation must be performed first as shown in eq.(20). With a hybrid

differencing scheme for the convective terms, $p = 1$ [2]. Thus, the truncation error estimation is evaluated by performing the explicit calculation in eq.(21).

$$\tilde{e}_h^\phi = \frac{\phi_h - \phi_{2h}}{2^p - 1} \quad (20)$$

$$\tilde{\tau}^\phi = \left(L_{x,h}^p [\phi_h + \tilde{e}_h^\phi] + S^\phi \right) \cdot (\Delta x \Delta y \Delta z) \quad (21)$$

5. Application to Turbulent Incompressible Cavity Flow

Turbulent incompressible cavity flow has been used as a benchmark solution to test the accuracy of the numerical solution. The geometry of a lid-driven cavity flow is illustrated in Figure 2. The dimension of each side is 0.15 m.

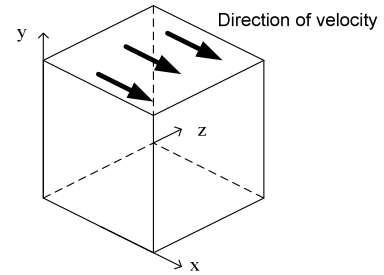


Figure 2. Geometry of 3D cavity flow.

The Reynolds number 3200 based on lid speed and cavity width is chosen as a test case here. The top of the cavity is moved with a uniform velocity. The grid sizes used are 20x20x20 and 40x40x40 control volumes for the double and base grids respectively, and the ratio of refinement is 2. The Gauss-Seidel is used as the iteration scheme. The truncation error is estimated on the base grid by the solution error equation (20) and then the truncation error equation (21). The refined regions occur where the truncation error is less than 1.0×10^{-11} as shown in Figure 3. In Figure 4, it shows the surface of the truncation error on the plane of symmetry.

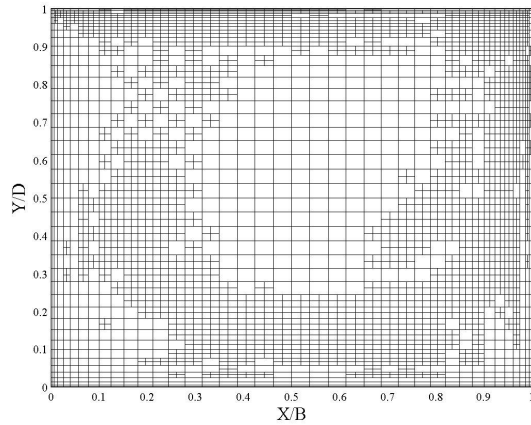


Figure 3. The local refined region on the plane of symmetry.

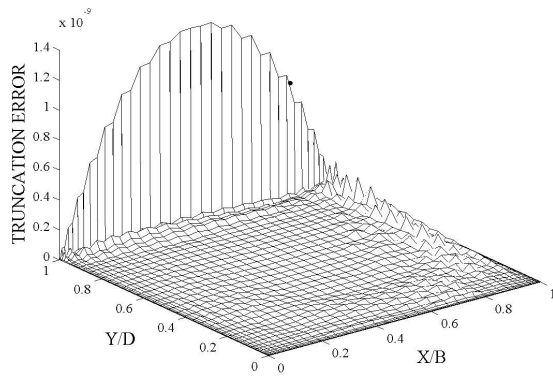


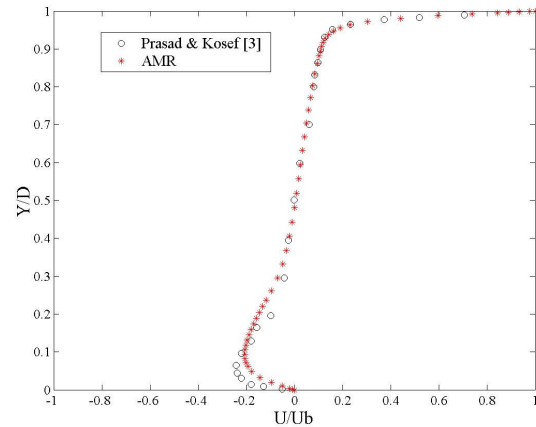
Figure 4. The truncation error on the plane of symmetry.

For the outer iteration, the interpolation is used to transfer the variable values from coarse to fine grids. The residuals of u -, v - and w -components on fine grid are restricted to the base grid only. All the properties are calculated with inner iteration until convergence. After that, the new solutions are interpolated from coarse to fine grids again so that the interface values are updated. If the maximum residual does not reach the criteria, this process will repeat until convergence.

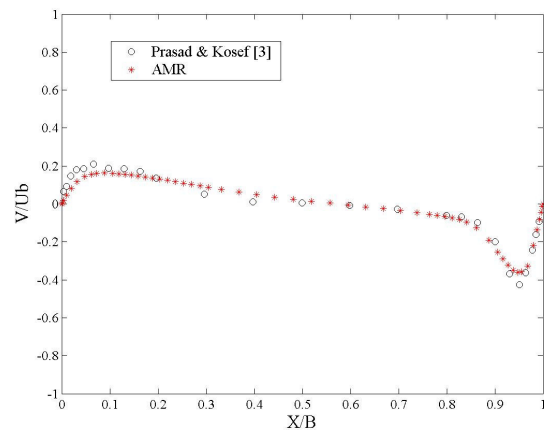
Figure 5 (A) and (B) illustrate the normalized streamwise and the normalized cross-stream velocities on the plane of symmetry respectively. It is seen that the computational results agree well with experimental data of Koseff and Prasad [3]. For the accuracy, Error Root Mean Square (ERMS) is used to present the accuracy of solution on each grid. In Table 1, the active calculation of turbulent incompressible cavity flow at $Re=3200$ has the same accuracy as non-uniform calculations at both grid sizes (40x40x40 and 80x80x80). In addition, the computing time of the adaptive mesh refinement is less than 10 times when compared with that of the finest uniform grid.

TABLE 1. Error Root Mean Square (ERMS)

Grid Size	ERMS	
	Non-Uniform	AMR
40x40x40	2.379×10^{-11}	2.124×10^{-11}
80x80x80	7.755×10^{-12}	1.769×10^{-14}



(A)



(B)

Figure 5. (A) Normalized streamwise velocity profile on the plane of symmetry.

(B) Normalized cross-stream velocity profile on the plane of symmetry.

6. Conclusion

An adaptive mesh refinement (AMR) method is a promising technique for solving the three-dimensional turbulent incompressible flow problem. The computer program is evaluated by using a lid-driven cavity flow as a test case. The present results agree well with the experimental data of Prasad and Koseff [3]. The resulting numerical solution is as accurate as non-uniform and non-uniform fine-grid calculations but use less computing time ten times less.

Acknowledgments

The present work is financially supported by Thailand Graduate Institute of Science and Technology (TGIST). This research is supported by the Thailand Research Fund (TRF) for the Senior Scholar Professor Dr. Pramote Dechaumphai. This support is greatly appreciated.

References

- [1] Berger, M. J. (1982). "Adaptive mesh refinement for hyperbolic partial differential equation," Ph.D. Thesis, Stanford University, USA.
- [2] Caruso, S. C. (1986). "Adaptive grid techniques for elliptic fluid-flow problems," Ph.D. Thesis, Stanford University, USA.
- [3] Prasad, A.K and Koseff, J.R. (1989). "Reynolds number and end-wall effects on a lid-driven cavity flow," *Physics of Fluids A*, 1(2)
- [4] Launder, B.E. and Sharma, B.I. (1974). "Application of the energy-dissipation model of turbulence to the calculation of flow near a spring disk," *Letters in Heat and Mass Transfer*, 1, 131-138.
- [5] Yu, D., Mei, R., and Shyy, W. (2002). "A multi-block lattice boltzmann method for viscous fluid flows," *The International Journal for Numerical Methods in Fluids*, 39, 99-120.
- [6] Martin, D., and Cartwright, K. (1998). "Solving poisson equation using adaptive mesh refinement," Lecture notes, <http://seesar.lbl.gov/anag/staff/martin/AMRPoisson/index.html>
- [7] Wilcox, D.C. (1993). "Turbulence modeling for CFD," DCW Industrial.
- [8] Sulak, S., Juntasaro, V., Uthayopas, P., and Juntasaro, E. (2003). "Fast solver for three-dimensional turbulent flow using multigrid method," *Proceedings of 7th Annual National Symposium on Computational Science and Engineering*, Faculty of Science, Chulalongkorn University, Bangkok, Thailand, March 24-26.
- [9] Sujit, E., Juntasaro, V., Uthayopas, P., and Juntasaro, E. (2003). "Numerical simulation of turbulent flow in

three-dimensional space." *Proceedings of 7th Annual National Symposium on Computational Science and Engineering*, Faculty of Science, Chulalongkorn University, Bangkok, Thailand, March 24-26.